Sensing and Bio-Sensing Research xxx (2016) xxx–xxx

Contents lists available at ScienceDirect

Sensing and Bio-Sensing Research

journal homepage: www.elsevier.com/locate/sbsr

Integration of microcoils for on-chip immunosensors based on magnetic nanoparticles capture

Olivier Lefebvre [a,*], Claire Smadja [b], Emile Martincic [a], Marion Woytasik [a], Mehdi Ammar [a]

[a] Centre de Nanosciences et de Nanotechnologies, CNRS, Univ. Paris-Sud, Université Paris-Saclay, C2N – Orsay, 91405 Orsay cedex, France
[b] Institut Galien Paris-Sud, CNRS UMR 8612, Université Paris Saclay, Chatenay-Malabry F-92296, France

ARTICLE INFO

Article history:
Received 1 July 2016
Received in revised form 12 October 2016
Accepted 22 October 2016
Available online xxxx

Keywords:
Bacteria
Lab-on-chip
ELISA
Magnetic nanoparticles
Ovalbumin
Microcoils
Fluorescent microscopy

ABSTRACT

Immunoassays using magnetic nanoparticles (MNP) are generally performed under the control of permanent magnet close to the micro-tube of reaction. Using a magnet gives a powerful method for driving MNP but remains unreliable or insufficient for a fully integrated immunoassay on lab-on-chip. The aim of this study is to develop a novel lab-on-chip concept for high efficient immunoassays to detect ovalbumin (Biodefense model molecule) with microcoils employed for trapping MNP during the biofunctionalization steps. The objectives are essentially to optimize their efficiency for biological recognition by assuring a better bioactivity (antibodies-ovalbumin), and detect small concentrations of the targeted protein (~10 pg/mL). In this work, we studied the response of immunoassays complex function of ovalbumin concentration. The impact of MNP diameter in the biografting protocol was studied and permitted to choose a convenient MNP size for efficient biorecognition. We realized different immunoassays by controlling MNP in test tube and in microfluidic device using a permanent magnet. The comparison between these two experiments allows us to highlight an improvement of the limit of detection in microfluidic conditions by controlling MNP trapping with a magnet.

1. Introduction

Biosensors could be defined by the need to incorporate a biological, biologically derived or biomimetic recognition element with a transducing element [1]. In a simple way a biological response has to be detected by a tool and converted in one way or another into an electrical signal.

Since the first publication of Enzyme-Linked Immune-Sorbent Assay (ELISA) by R. S. Yalow in 1960 [2], the ELISA method has been used as a diagnostic tool in biology and medicine and it became one of the most specific method in immunoassay for Alzheimer diseases [3], HIV virus detection [4] or cancerous biomarker [5,6]. Particularly this technic allows a detection of low concentration. Conventionally ELISA method is performed in wells or tube. Three type of ELISA can be found direct ELISA, sandwich ELISA and competitive ELISA but a prepared surface is needed for all.

Another complementary method to ELISA has emerged using magnetic nano or micro beads [7] which are functionalized in fluidic conditions [8]. Since few years, the use of functionalized beads by trapping them in a magnetic field had opened the route to on-chip bead-based ELISA system. In fact, a higher sensitivity is obtained using micro-nano beads to increase surface to volume ratio combined with microfluidic devices [9,10].

Using MNP is a common way to realize immunoassay [11–14]. In this topic, MNP have really interesting properties such as (i) specific functionalization, (ii) easy manipulation, (iii) an important specific surface (surface/volume ratio) which offers us a better condition for biografting [15]. MNP are useful to realize an immunoassay on chip [12,16], by blocking them with magnetic field and injecting continuous flow with different solutions [9]. Another alternative consists on moving nano-beads through different solutions which permit to realize dynamic immunoassay [17].

Microfluidic devices are largely developed, in different domains, for instance (i) quantification [18,19] (ii) cell analysis [7,20]. Many functions such as sensing, mixing, manipulation [21–23], could be integrated on microfluidic devices with one aim to build a lab-on-chip environment. Microfluidic device can be made of PDMS (PolyDimethyl Siloxane). It is a silicone elastomer with desirable properties that make it attractive for microfluidic components and biomedical application. In fact, PDMS ensures thermal stability, permeability to gases, easiness for handling and manipulating [24]. These properties allow a rapid and low cost fabrication of microfluidic devices.

Nowadays ELISA using nanoparticles to detect pathogen bacteria [25] is extensively applied for food poisoning [26,27] since it was considered as a major health threat by governments and other applications are also pursued [28–30]. This specific ELISA method demonstrates that a very low limit of detection could be reached with a high level of sensitivity.

* Corresponding author.
E-mail address: olivier.lefebvre@u-psud.fr (O. Lefebvre).

http://dx.doi.org/10.1016/j.sbsr.2016.10.008

The objective of this work is to integrate microcoils in a fluidic system in order to validate the concept of immunoassay formation and MNP trapping and detection by microcoils. In fact, in this paper we present one part of our work concerning the integration of immunoassay in microfluidic system which involves permanent magnet for MNP capture. The next step will be to implement microcoils of trapping and detection in a conveniently designed lab-on-chip.

2. Principle of magnetic trapping

MNP can be manipulated and controlled in fluidic device by a magnetic field created by a magnet or microcoils for instance [31–33].

As it known, when a particle is localized in a magnetic field $\overrightarrow{H_a}$, it obtains a magnetic moment aligned in the magnetic field direction:

$$\overrightarrow{M_p} = \chi \overrightarrow{H_a} \tag{1}$$

$\overrightarrow{M_p}$ as magnetic susceptibility and χ as magnetic moment per volume unit. We can distinguish two types of susceptibility: (i) intrinsic magnetic susceptibility χ_p which is the ratio of the magnetization to the applied field (ii) measured magnetic susceptibility χ_m which is the ratio of the magnetization to the local magnetic field inside the particle. Besides an equivalent bipolar moment $\overrightarrow{M_p}$ is usually obtained to calculate the magnetic force:

$$\overrightarrow{m_p} = \frac{3\chi_p(\chi_m+1)}{\left[\left(\chi_p-\chi_m\right)+3(\chi_m+1)\right]}\overrightarrow{H_a}. \tag{2}$$

Magnetic field creates magnetic force to control MNP. Magnetic force can be described as:

$$\overrightarrow{F_{mp}} = \left(\vec{m}.\vec{\nabla}\right).\vec{B} \tag{3}$$

$\overrightarrow{m}$ as the equivalent dipolar magnetic moment of each particles. When magnetic particles are suspended in a fluid, where μ_f is the permeability, the relation between $\vec{B}$ and $\overrightarrow{H_a}$ can be described as:

$$\vec{B} = \mu_f \overrightarrow{H_a} \tag{4}$$

If we assumed that the magnetization is linear, and according to Eqs. (2) and (4) the magnetic force acting on magnetic particle can be described as:

$$\overrightarrow{F_{mp}} = \mu_f V_p \frac{3\left(\chi_p-\chi_m\right)}{\left[\left(\chi_p-\chi_m\right)+3(\chi_m+1)\right]}\left(\overrightarrow{H_a}.\nabla\right)\overrightarrow{H_a} \tag{5}$$

V_p as the volume of a particle. We can extract from Eq. (5) two cases: $\chi_p > \chi_m$ where the particles will be under an attractive force and $\chi_p < \chi_m$ where the particles will be under a repulsive force. Magnetic force can be used to attract and repulse magnetic particles and the strong of the force depend of several parameters including magnetic field and parameters of the particle.

Regarding this consideration, simulations have been performed on ANSYS® software to define the convenient design of microcoils for efficient MNP trapping. Indeed, in this paper we present microcoils with the following optimized parameters: 45 turns, width of Copper wires = 10 μm, distance between wires = 10 μm, height of wire = 10 μm, outer radius of the coil = 5 mm (Fig. 3).

3. Principle of immunoassay sandwich involving magnetic nanoparticles

The enzyme-linked immunosorbent assay (ELISA) is a test that uses antibodies to detect the presence of a substance (target), usually a biomarker, in a liquid sample or wet sample.

Ovalbumin is used as a model molecule for biodefense and as target for the developed ELISA protocol in this work. The principle is to encapsulate the target (a biomarker) between two antibodies and one antibody for the detection. Primary antibody recognises a part (epitope) of the biomarker, the second antibody recognises another epitope of the biomarker. The detection antibody recognises a part of the second antibody and the resulting structure forms the biological complex (immunoassay sandwich, Fig. 1b). This complex is completed by a magnetic nanoparticle where the primary antibody is grafted with an EDC/NHS protocol at 4 °C, Fig. 1a.

In addition, BSA is used to avoid the non-specific absorption of biological elements, this step is performed after the primary antibodies grafting to fill up free surface between antibodies. As it shows in Fig. 1c, a monolayer of antibodies could be grafted on one magnetic nanoparticle therefore several biological complex could be observed.

4. Material and methods

4.1. Material and experimental equipment

A microfluidic platform is used to perform immunoassay according an ELISA protocol. A fluidic pump and a syringe are used to inject fluid inside the microfluidic system. A Peltier module with an electrical equipment and a temperature sensor are used to regulate the temperature during experiments. A fluorescent microscope (Euromex Série B) with 4x NeoLED™ for monochromatic LED Epi-Fluorescence and standard filters (Green EX 460–550 nm EM 590 nm) is used to visualize fluorescent antibodies.

The microfabrication of microfluidic devices and microcoils are made in a clean room. Two types of 4 in. wafers are used, silicon wafer and glass wafer.

Different equipment are used for microfabrication: UV-photolithography EVG 620 for print panel on photoresist. Electrolyte bath using Cu_2SO_4 and H_2SO_4 with integrated electrode of copper for electrodeposition of copper. Denton sputtering system (EXPLORER Denton Vacuum® system) and PECVD (STS PECVD System) for depositing layer. Reactive Ion Etching (STS RIE system) and Ion Beam Etching (IBE Roth & Rau IonSys 500) for etching layer. DEKTAK 8 (Veeco) and Keyence microscope for characterization.

MNP with carboxylic terminal group are purchased from Adamtech © (Carboxyl-Adembeads and MasterBeads Carboxylic Acid) and are cleaned with NaOH 1 mM solution for one day.

Biological and chemical material are used in ELISA protocol: EDC/NHS (*N*-(3-Dimethylaminopropyl)-*N*′-ethylcarbodiimide/*N*-hydroxysulfosuccinimide from Sigma-Aldrich ©) for grafting. Primary antibodies: Rabbit Anti-Ovalbumin (Hen White) from Merck Millipore ©. BSA (Bovine Serum Albumin) from Sigma-Aldrich © for passivation. Ovalbumin (Albumin from chicken egg white) from Sigma-Aldrich ©. Secondary antibodies: Purified anti-chicken ovalbumin from BioLegend ©. Detection antibodies: Anti-mouse IgG (Fab specific)-FITC antibody produced in goat from Sigma-Aldrich ©. PEO solution (Poly(ethylene oxide) from Sigma-Aldrich ©).

4.2. Microfabrication

4.2.1. Microfluidic on glass wafer

Microfluidic devices are composed of two parts: glass wafer with a thin layer of PDMS (20 μm) spin-coated on it and fluidic channels made of PDMS. A schematic illustration of the process is presented in Fig. 2a.

Please cite this article as: O. Lefebvre, et al., Integration of microcoils for on-chip immunosensors based on magnetic nanoparticles capture, Sensing and Bio-Sensing Research (2016), http://dx.doi.org/10.1016/j.sbsr.2016.10.008

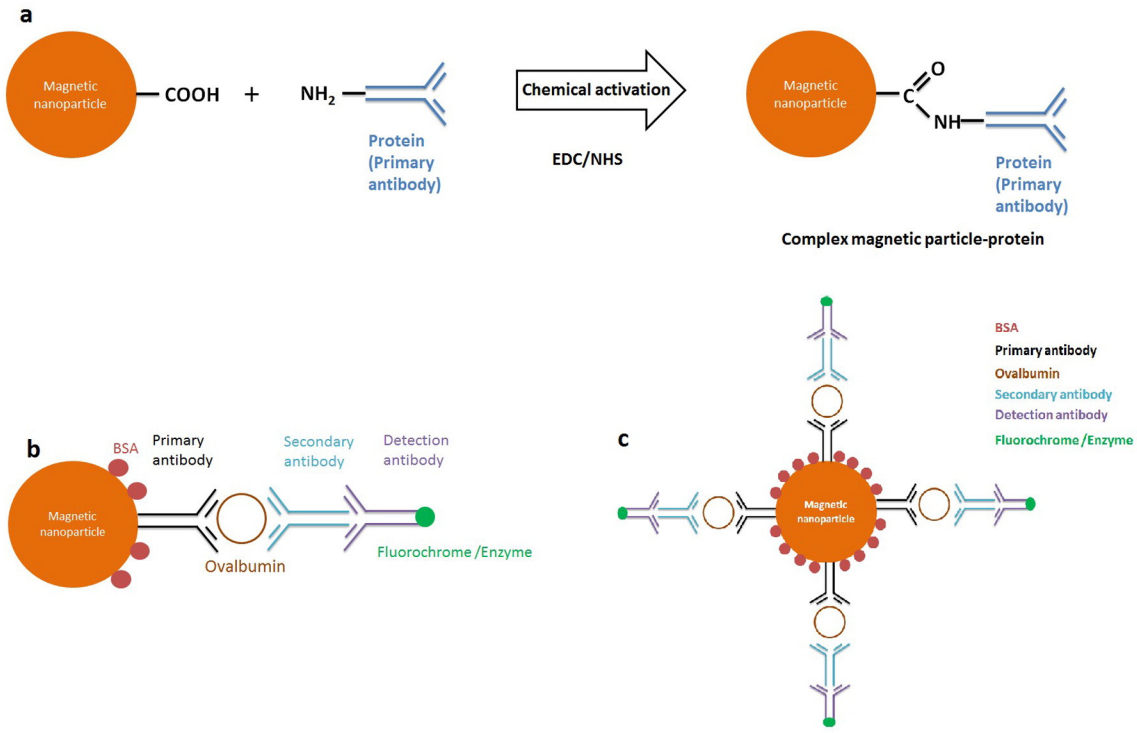

Fig. 1. (a) EDC/NHS grafting protocol; schema of (b) one grafted immunocomplex; (c) magnetic nanoparticle with a layer of grafted immunocomplex.

First, a master mold on silicon wafer is made to replicate the fluidic system. A 50 μm layer of SU8 2050 is spin coated on a clean silicon wafer (Fig. 2a.2). A step of UV-photolithography is realized to obtain the channel form (Fig. 2a.3). UV-photolithography conditions were soft-contact and an energy of 250–260 mJ/cm^2. The height of the master mold is systematically verified using a mechanical profilometer (DEKTAK). The fabricated channel has systematically 50 μm of height and 500 μm of wide.

PDMS is formed by the mixture of two solutions: silicon elastomer and curing agent. We optimized the properties of the PDMS structured which will ensure the best robustness of the fluidic system. In this optic, we used a standard ratio 10 (silicon elastomer) per 1 (curing agent). PDMS is poured on the master mold and baked 2 h at 75 °C in an oven to obtain a replica (Fig. 2a.4). The replica is unmold and inlet and outlet are made (Fig. 2a.5). The PDMS replica is bonded by an O_2 plasma on the prepared glass wafer (Fig. 2a.6 & 7 & b). Bonding conditions were a power of 160 W with a pressure of O_2 at 0.4 mbar and one minute time.

Microfluidic system on silicon wafer.

In silicon wafer, twenty microcoils are fabricated in a clean room using a mastered process [34], a schematic illustration of the process is presented in Fig. 3a.

First, the wafer is clean by Piranha (mix of sulfuric acid and hydrogen peroxide) and BHF (Buffer HF) solution (Fig. 3a.1). Then a thin layer (200 nm) of silicate is deposited using an oxidation oven (Fig. 3a.2). A seed layer of 100 nm of copper and 10 nm of titanium is added using a cathode pulverization (Fig. 3a.3), conditions are for Titanium layer: current of 200 mA for 600 s and then current of 276 V and a pressure of 8 μbar for 200 s; for the copper layer: current of 400 mA for 200 s and then current of 335 V and a pressure of 8 μbar for 200 s. A step of UV-photolithography is made using an AZ4562 photoresist (Fig. 3a.4 &

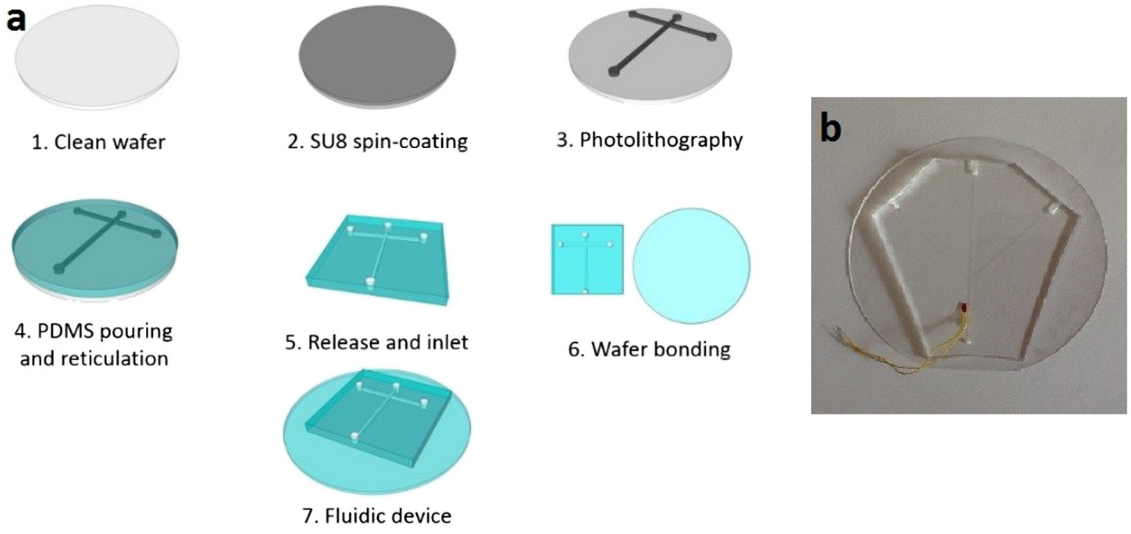

Fig. 2. (a) Illustration: microfabrication steps of microfluidic device; (b) photography of microfluidic device.

Please cite this article as: O. Lefebvre, et al., Integration of microcoils for on-chip immunosensors based on magnetic nanoparticles capture, Sensing and Bio-Sensing Research (2016), http://dx.doi.org/10.1016/j.sbsr.2016.10.008

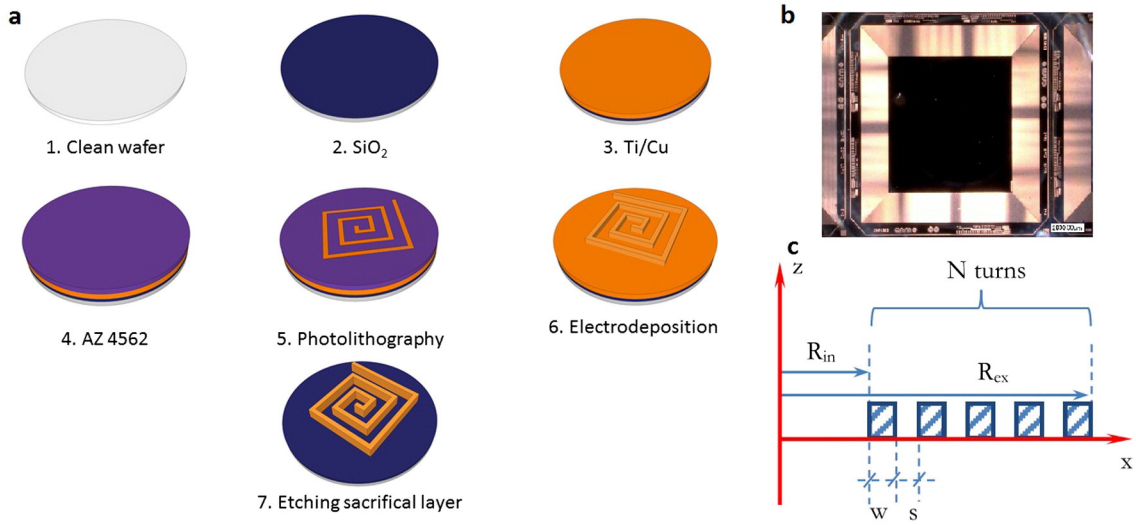

Fig. 3. (a) Summary of microfabrication steps of microcoils; (b) photography of one microcoil; (c) schematic view of microcoils N: 45 turns, w: width of wires = 10 μm, s: distance between wires = 10 μm, R_{ex}: outer radius of the coil = 5 mm, R_{in}: inner radius of the coil = 3 mm.

5), conditions were soft-contact and an energy of 365 mJ/cm^2. We electrodeposited a 10 μm layer of copper using a specific bath with integrated electrodes (Fig. 3a.6) and we etched the sacrificial layer (Fig. 3a.7). We diced the wafer to separate microcoils (Fig. 3b).

Finally, to integrate microcoil in the microfluidic device we stick it on a PCB board and a wire-bonding is done using an aluminium wire. An electrical connection is realized to connect microcoil to an input current. Microcoils are recovered with a 10 μm PDMS layer (proportion 2.5:1, optimized for convenient soft covering of wires) to protect and to prepare the O_2 plasma bonding with the microfluidic channel part.

4.3. ELISA protocol description

In test tube, an EDC/NHS protocol, 24 h at 4 °C, is performed to grafted primary antibodies on MNP (Fig. 4b). BSA is added, to protect MNP from non-specific absorption, during two hours at room temperature (Fig. 4c). Ovalbumin which is the target is added (different concentrations are tested) during two hours at room temperature (Fig. 4d). Secondary antibodies are added during two hours (Fig. 4e) at room temperature and finally detection antibodies are added during two hours at room temperature (Fig. 4f). After each pre-defined step a washing step, using a magnet to block MNP, is done to remove all biological elements which are not grafted. Finally, the functionalized MNP are observed on glass under the fluorescent microscope.

In a microfluidic system the ELISA protocol remains mostly the same, a step of channel protection is added and step times are reduced considerably (Fig. 4g).

First PDMS channels are protected from unwanted absorption of biological elements (antibodies, antigen) using an HCl/PEO protocol (Fig. 5). After the O_2 plasma (Fig. 5b) bonding the input and the output of the microfluidic device are blocked to keep the activation. A 1 M HCl solution is injected at 10 μL/min in order to protonating silanol groups on PDMS surface (Fig. 5c & d), and then a PEO solution is injected to graft PEO chains on PDMS surface (Fig. 5e & f). After cleaning the device with PBS buffer, ELISA protocol as described previously is used. As expected, the step times are reduced, due to the confinement of the reaction on fluidic condition. The EDC/NHS protocol decreased from 24 h to 30 min but remains at 4 °C using the temperature regulator. Next steps are decreased from two hours to 10 min and we used the temperature regulator to keep the temperature constant (22 °C to optimize the reproducibility). Washing step can be realized at a more powerful flow rates, than biological step, regarding the ratio between the microfluidic and the magnetic force. Finally the input and output are blocked to avoid leaks of fluids and then results are observed using a fluorescent microscope.

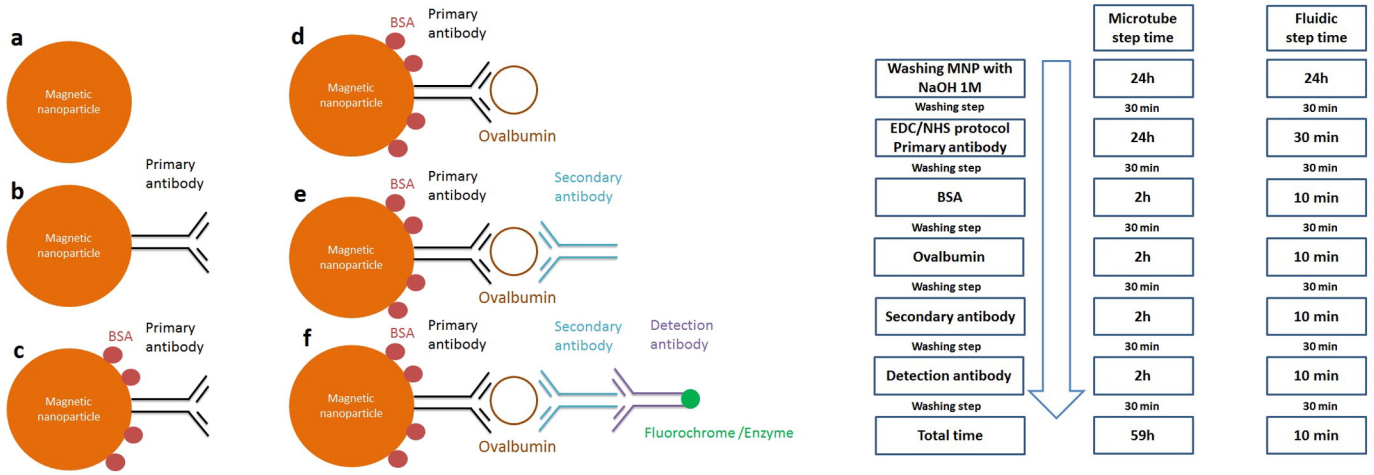

Fig. 4. (a–f) Schematic ELISA protocol; (g) protocol time step of test in microtube and in fluidic condition.

Please cite this article as: O. Lefebvre, et al., Integration of microcoils for on-chip immunosensors based on magnetic nanoparticles capture, Sensing and Bio-Sensing Research (2016), http://dx.doi.org/10.1016/j.sbsr.2016.10.008

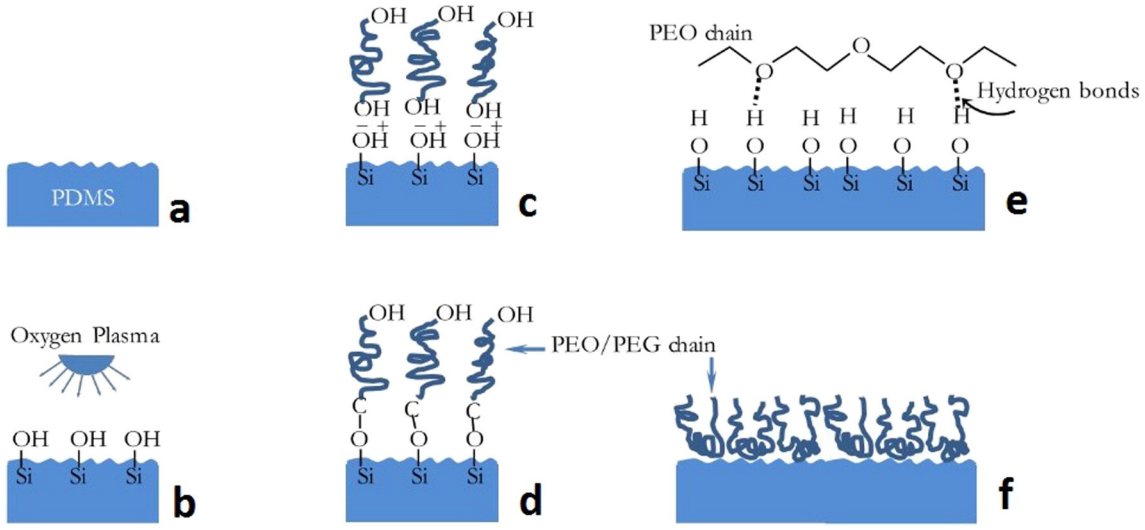

Fig. 5. Principles of covalent and adsorptive attachment of PEO. (a) Native surface of PDMS; (b) high density of silanol groups on the surface are produced by plasma treatment; (c–d) silanol groups react with the terminal group of PEO; (e–f) physical and chemical absorption of PEO chains generates a polymer layer in PDMS surface.

4.4. Fluorescent images processing

The fluorescent characterization is carried out through the channels of the microfluidic device. For one concentration of the target (ovalbumin) the experiment is realized several times (minimum 3 times). The result is obtained by fluorescent microscope imaging. Several images are needed to observe all the detection area to validate that maximum of complexes are characterized.

Each image is processed using a home-made developed program. First a thresholding is applied for top and low values to avoid any artefact. The background noises are deleted using the comparison of an experiment without ovalbumin (control experiment). Too big luminescent responses related to the aggregations of MNP or antibodies are eliminated. Finally the intensity of one image I_{image} is extracted. For one channel the intensity calculated $I_{channel}$ is the average of the intensities (I_{image}) of each image from the channel. And for one concentration of the ovalbumin the intensity calculated $I_{concentration}$ is the average of the $I_{channel}$ of the same concentration.

5. Results and discussion

5.1. Immunoassay complex validation

The first investigation concerns the grafting step of the antibody layer on the biological process. We need to demonstrate that if we skip a step (EDC/NHS protocol step, the ovalbumin step and the detection antibody step) on the protocol, the complex formation is not validated in final. These experiments were realized in tube and in the microfluidic device. Images presented in this paper were extracted from experiments in microfluidic device. We can see a successful immunoassay (Fig. 6a) and unsuccessful immunoassays (Fig. 6b–d). A study on the protection of PDMS from aggregation of biological element was realized by removing the HCl/PEO protocol, the results with the emergence of aggregation phenomena are presented in Fig. 6e.

In conclusion we demonstrate that without primary antibody (Fig. 6b), ovalbumin (Fig. 6c) or detection antibody (Fig. 6d), immunoassay

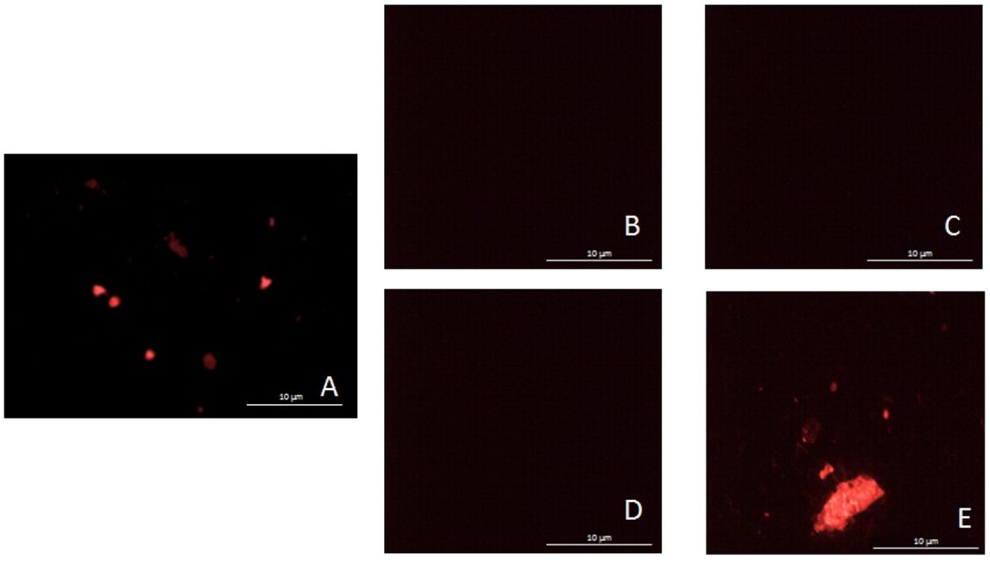

Fig. 6. (a) Whole biografting process is respected; we skipped (b) the primary antibody grafting step; (c) the ovalbumin grafting step; (d) the detection antibody grafting step; € channel without PDMS protection by HCl/PEO.

Please cite this article as: O. Lefebvre, et al., Integration of microcoils for on-chip immunosensors based on magnetic nanoparticles capture, Sensing and Bio-Sensing Research (2016), http://dx.doi.org/10.1016/j.sbsr.2016.10.008

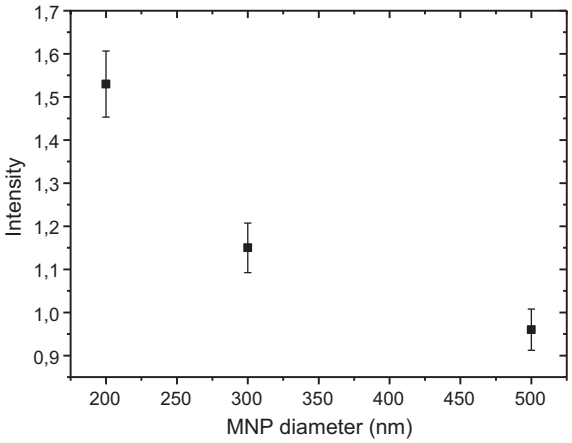

Fig. 7. Intensity of the response of immunoassay extracted from test using different size of magnetic nanoparticles.

was unsuccessful and without HCl/PEO treatment, aggregations of MNP and antibodies were appearing.

5.2. Influence of magnetic nanoparticles diameter

The second study concerns the influence of the MNP diameter. We showed in part 2 that the magnetic force is depending of the magnetic field and MNP properties. In fact if we decrease the size of the MNP we need to increase the magnetic field to have a constant magnetic force. In the other hand MNP have a behavior that follows specific surface formulas (6), (7) and (8). In particular, we can conclude that the specific surface decreases with the diameter of the MNP.

$$V_{sphère} = \frac{4\pi R^3}{3} \tag{6}$$

$$A_{sphère} = 4\pi R^2 \tag{7}$$

$$\chi_{A/V} = \frac{3}{R} \tag{8}$$

In this optic, we performed experiments with MNP of 200 nm, 300 nm and 500 nm diameter. For each experiment we use the same volume of MNP (10 μL) and all the step remain the same. The results in Fig. 7, confirm the dependence of the grafting on the specific surface. In other hand, to limit the thermal Joule effect when we inject current in microcoils of trapping of MNP we need to avoid a very low size of nanoparticles which required a very high magnetic field to control them. Indeed, we eliminated the size of 200 nm and a diameter of 300 nm was selected regarding the magnetic force needed and the intensity detected.

5.3. Influence of ovalbumin concentration immunoassay response function

The final study presented in this paper concerns the immunoassay response, involving the 300 nm MNP, function of ovalbumin concentration. It should give us information about the limit of detection (L.O.D) that can be reached. The L.O.D. is determined using the formula:

$$L.O.D. = I_0 + 3 * \sigma_D \tag{4}$$

σ_D: standard deviation and I_0: intensity with no target. Our aim is to obtain the minimum intensity detectable which permit us to access to ovalbumin concentration that we can detect. The first analysis concerns the test in microtubes which are easier to manipulate then in microfluidic device with a permanent magnet.

We realized immunoassay using protocol in test tube as describe in 3 and we varied the concentration of ovalbumin from 0 μM to 15 μM (Fig. 8a). The curve shows us two parts: the first from 0 to 4 μm which corresponds to the enhancement of the biological complex quantity developed on the surface of MNP. The second one from 4 to 15 μM corresponds to a plateau when all or most bioactive sites have been occupied by a biological complex. The L.O.D. obtained by the formula (4) is 1.2 nM.

As in microtubes we followed the same protocol for microfluidic device as described in the part Section 4.3. We used a permanent magnet below the microfluidic channels to control MNP. We also realized the experiments for the same concentrations of ovalbumin (Fig. 8b) to compare the two ELISA environments of experimentation (in microtube and microfluidic conditions). As described in the part Section 3, the microfluidic device allows us not only to save considerably the time reaction but also to reach a better L.O.D. close to 0.3 nM.

In conclusion an improved limit of detection was confirmed (divided by 4) for integrated immunoassay of ovalbumin detection compared to those in microtube environment, essentially by controlling the MNP trapping with a magnet in microfluidic conditions.

6. Conclusion

We developed an original and innovative fully-integrated immunoassay on lab-on-chip in order to detect bacteria. We use ovalbumin as a Biodefense model biomarker, magnetic nanoparticles and ELISA protocol to perform immunoassay. We demonstrate the advantage of microfluidic environment by reducing grafting and preparation time and optimizing the limit of detection (less four times than microtube test).

By introducing microcoils in fluidic condition, we hope to obtain a fully integrated lab-on-chip which should allow us to attain optimal

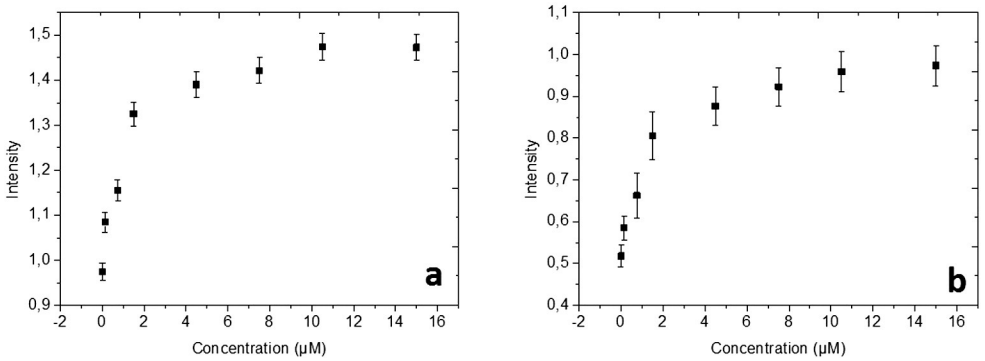

Fig. 8. Fluorescent intensity of immunoassay response function of ovalbumin concentration: (a) in microtubes; (b) in microfluidic devices.

Please cite this article as: O. Lefebvre, et al., Integration of microcoils for on-chip immunosensors based on magnetic nanoparticles capture, Sensing and Bio-Sensing Research (2016), http://dx.doi.org/10.1016/j.sbsr.2016.10.008

specificity and sensitivity for the detection of very low bacteria concentration for biodefense applications.

Acknowledgements

This work was supported by French National Agency of Research ANR-DGA-13-ASTR-0021 AMMIB (Multimodal Analysis Integrated for Biodefense) http://www.agence-nationale-recherche.fr/?Project=ANR-13-ASTR-0021.

References

[1] J.P. Lafleur, et al., Recent advances in lab-on-a-chip for biosensing applications, Biosens. Bioelectron. 76 (2015) 213–233.
[2] B.R.S. Yalow, S.A. Berson, Immunoassay of endogenous plasma insulin in man, J. Clin. Invest. 39 (1960) 1157–1175.
[3] C.M.C.L.-S. Wag, Y.Y. Leung, S.-K. Chang, S. Leight, M. Knapik-Czajka, Y. BAek, L.M. Shaw, V.M.Y. Lee, J.Q. Trojanowwski, Comparison of xMAP and ELISA assays for detecting CSF biomarkers of Alzheimer's disease, J. Alzheimers Dis. 31 (2012) 439–445.
[4] T.K.M. Honda, S. Yamamoto, M. Cheng, K. Yasukawa, H. Suzuki, T. Saito, Y. Osugi, T. Tokunaga, Human soluble IL 6 receptor its detect and enhanced release by HIV infection, J. Immunol. 148 (1992) 2175–2180.
[5] R. Ahmad, W.J. Ellis, A.Y. Liu, E.A. Wayner, S. Quek, R. Ahmad, M.E. Ho, L.D. True, A.Y. Liu, Development of an ELISA to detect the secreted prostate cancer biomarker AGR2 in voided urine development of an ELISAto detect the secreted prostate cancer biomarker AGR2 invoided urine, Prostate 72 (2012) 1023–1034 (no. June).
[6] N.U.N. Scholler, M. Crawford, A. Sato, C.W. Drescher, K.C. O'Briat, N. Kiviat, G.L. Anderson, Bead based ELISA assays for validation of ovarian cancer early detection markers, Clin. Cancer Res. 12 (2006) 2117–2124.
[7] H.-Y. Cheng, L.-J. Lai, F.-H. Ko, Rapid and sensitive detection of rare cancer cells by the coupling of immunomagnetic nanoparticle separation with ELISA analysis, Int. J. Nanomedicine 7 (2012) 2967–2973.
[8] K.S. Kim, J. Park, Magnetic force-based multiplexed immunoassay using superparamagnetic nanoparticles in microfluidic channel, Lab Chip 5 (2005) 657–664.
[9] D.J.B. Bechstein, J.-R. Lee, C.C. Ooi, A.W. Gani, K. Kim, R.J. Wilson, S.X. Wang, High performance wash-free magnetic bioassays through microfluidically enhanced particle specificity, Sci. Rep. 5 (2015) 11693 (no. February).
[10] Q. Ramadan, V. Samper, D. Poenar, C. Yu, On-chip micro-electromagnets for magnetic-based bio-molecules separation, J. Magn. Magn. Mater. 281 (2–3) (2004) 150–172.
[11] F. Lacharme, C. Vandevyver, M.A.M. Gijs, Magnetic beads retention device for sandwich immunoassay: comparison of off-chip and on-chip antibody incubation, Microfluid. Nanofluid. 7 (2009) 479–487.
[12] H. Park, M.P. Hwang, K.H. Lee, Immunomagnetic nanoparticle-based assays for detection of biomarkers, Int. J. Nanomedicine 8 (2013) 4543–4552.
[13] A. Ranzoni, G. Sabatte, L.J. Van Ijzendoorn, M.W.J. Prins, One-step homogeneous magnetic nanoparticle immunoassay for biomarker detection directly in blood plasma, ACS Nano (4) (2012) 3134–3141.
[14] X. Xie, N. Ohnishi, Y. Takahashi, A. Kondo, Application of magnetic nanoparticles in full-automated chemiluminescent enzyme immunoassay, J. Magn. Magn. Mater. 321 (2009) 1686–1688.
[15] L.H. Reddy, J.L. Arias, J. Nicolas, P. Couvreur, Magnetic nanoparticles: design and characterization, toxicity and biocompatibility, pharmaceutical and biomedical applications, Chem. Rev. 112 (2012) 5818–5878.
[16] A. Van Reenen, A.M. De Jong, M.J. Den Toonder, Integrated lab-on-chip biosensing systems based on magnetic particle actuation - a comprehensive review, Lab Chip 15 (2014) 1966–1986.
[17] S.A. Peyman, A. Iles, N. Pamme, Rapid on-chip multi-step (bio)chemical procedures in continuous flow—manoeuvring particles through co-laminar reagent streams, Chem. Commun. (Camb.) (10) (2008) 1220–1222.
[18] R. Sista, Z. Hua, P. Thwar, A. Sudarsan, V. Srinivasan, A. Eckhardt, M. Pollack, V. Pamula, Development of a digital microfluidic platform for point of care testing, Lab Chip 8 (12) (2008) 2091.
[19] S.V. Pereira, G.A. Messina, J. Raba, Integrated microfluidic magnetic immunosensor for quantification of human serum IgG antibodies to Helicobacter pylori, J. Chromatogr. B 878 (2) (2010) 253–257.
[20] S.-Q. Gu, Y.-X. Zhang, Y. Zhu, W.-B. Du, B. Yao, Q. Fang, Multifunctional picoliter droplet manipulation platform and its application in single cell analysis, Anal. Chem. 83 (19) (2011) 7570–7576.
[21] A.D. Henriksen, G. Rizzi, F.W. Østerberg, M.F. Hansen, Optimization of magnetoresistive sensor current for on-chip magnetic bead detection using the sensor self-field, J. Magn. Magn. Mater. 380 (2015) 209–214.
[22] A.H.C. Ng, K. Choi, R.P. Luoma, J.M. Robinson, A.R. Wheeler, A. Diagnostics, A.P. Road, A. Park, U. States, Digital micro fluidic magnetic separation for particle-based immunoassays, Anal. Chem. 84 (2012) 8805–8812.
[23] R. Afshar, Y. Moser, T. Lehnert, M.A.M. Gijs, Magnetic particle dosing and size separation in a microfluidic channel, Sensors Actuators B Chem. 154 (1) (2011) 73–80.
[24] A. Mata, A.J. Fleischman, S. Roy, Characterization of polydimethylsiloxane (PDMS) properties for biomedical micro/nanosystems, Biomed. Microdevices 7 (4) (2005) 281–293.
[25] S. Agrawal, K. Paknikar, D. Bodas, Development of immunosensor using magnetic nanoparticles and circular microchannels in PDMS, Microelectron. Eng. 115 (2014) 66–69.
[26] I. Cho, J. Irudayaraj, In-situ immuno-gold nanoparticle network ELISA biosensors for pathogen detection pathogen detection, Int. J. Food Microbiol. 164 (2013) 70–75.
[27] X. Jiang, R. Wang, Y. Wang, X. Su, Y. Ying, J. Wang, Y. Li, Evaluation of different micro/nanobeads used as amplifiers in QCM immunosensor for more sensitive detection of E. coli O157: H7, Biosens. Bioelectron. 29 (1) (2011) 23–28.
[28] J.C. Vidal, J.R. Bertolín, L. Bonel, L. Asturias, M.J. Arcos-martínez, J.R. Castillo, Rapid determination of recent cocaine use with magnetic particles-based enzyme immunoassays in serum, saliva, and urine fluids, J. Pharm. Biomed. Anal. 125 (2016) 54–61.
[29] Y. Ding, T. Cong, X. Chu, Y. Jia, X. Hong, Y. Liu, Magnetic-bead-based sub-femtomolar immunoassay using resonant Raman scattering signals of ZnS nanoparticles, Anal. Bioanal. Chem. (2016) 5013–5019.
[30] S. Schrittwieser, B. Pelaz, W.J. Parak, S. Lentijo-mozo, K. Soulantica, J. Dieckhoff, F. Ludwig, A. Guenther, A. Tschöpe, J. Schotter, Homogeneous biosensing based on magnetic particle labels, Sensors 16 (6) (2016).
[31] Q. Cao, X. Han, L. Li, Configurations and control of magnetic fields for manipulating magnetic particles in microfluidic applications: magnet systems and manipulation mechanisms, Lab Chip 14 (15) (2014) 2762–2777.
[32] A.E. David, A.J. Cole, B. Chertok, Y.S. Park, V.C. Yang, A combined theoretical and in vitro modeling approach for predicting the magnetic capture and retention of magnetic nanoparticles in vivo, J. Control. Release 152 (1) (2011) 67–75.
[33] M.M. Larimi, A. Ramiar, A.A. Ranjbar, Numerical simulation of magnetic nanoparticles targeting in a bifurcation vessel, J. Magn. Magn. Mater. 362 (2014) 58–71.
[34] M. Woytasik, J. Moulin, E. Martincic, A.-L. Coutrot, E. Dufour-Gergam, Copper planar microcoils applied to magnetic actuation, Microsyst. Technol. 14 (7) (2007) 951–956.

Please cite this article as: O. Lefebvre, et al., Integration of microcoils for on-chip immunosensors based on magnetic nanoparticles capture, Sensing and Bio-Sensing Research (2016), http://dx.doi.org/10.1016/j.sbsr.2016.10.008